Research paper

Pressure-induced structural phase transition and dehydration for gypsum investigated by Raman spectroscopy and electrical conductivity

Linfei Yang [a,b], Lidong Dai [a,*], Heping Li [a], Haiying Hu [a], Yukai Zhuang [a,b], Kaixiang Liu [a,b], Chang Pu [a,b], Meiling Hong [a,b]

[a] Key Laboratory of High-Temperature and High-Pressure Study of the Earth's Interior, Institute of Geochemistry, Chinese Academy of Sciences, Guiyang, Guizhou 550081, China
[b] University of Chinese Academy of Sciences, Beijing 100049, China

ARTICLE INFO

ABSTRACT

The structural phase transition and dehydration for gypsum were investigated by Raman spectroscopy and electrical conductivity up to ~12.2 GPa and ~723 K. A ~5.8 GPa of phase transition was verified at atmospheric temperature. The variations in the sulfate and hydroxyl Raman shifts and a change in electrical conductivity marked the onset of dehydration. At ~2.5 GPa, gypsum transformed into bassanite at ~523 K, and then completely dehydrated to γ-anhydrite at ~673 K. And furthermore, the gypsum-bassanite and bassanite-anhydrite dehydration boundaries were obtained: P (GPa) = −23.708 + 0.050 T (K) and P (GPa) = −4.907 + 0.011 T (K), respectively.

© 2018 Elsevier B.V. All rights reserved.

1. Introduction

Gypsum is a common hydrous mineral often occurring in hydrothermal vents near mid-ocean ridges, altered marine sediments and evaporite deposits, and its presence on Mars is an important indication for the existence of water in the planet's history [1]. The dehydration product from gypsum to anhydrite was observed as a form of the Nano-inclusion in diamond at a correspondent mantle pressure of 3–10 GPa [2]. It implies that gypsum may endure a dehydration reaction in the process of mantle subduction and accompany to release a large quantity of water-bearing fluids into the deep mantle. Previously reported results have confirmed that these water-bearing (salinity-bearing) fluids released from the dehydration of hydrous minerals explain the occurrence of earthquake and the high electrical conductivity anomaly in subduction zone [3–5]. And therefore, it is crucial to have a detailed knowledge of the physical and chemical properties of gypsum under high temperature and pressure.

The high-pressure vibrational and structural properties of gypsum have been previously investigated at ambient temperature by Raman and infrared spectroscopy, X-ray diffraction and first-principles calculations [6–9]. All of these results revealed a reversible phase transition from gypsum-I to gypsum-II at the pressure range of 4.0–6.0 GPa. As usual, it is believed that the occurrence of structural phase transition is accompanied by the variation of electronic structure at the same time. And whereas, the pressure-induced structural transformation can be efficiently checked by the electrical conductivity measurement of sample. To the best of our knowledge, the high-pressure electrical properties of gypsum have not been reported at room temperature till now.

As a representative hydrous mineral for gypsum, it is well known that the phenomenon of dehydration reaction may be widely existed at conditions of high temperature and high pressure. There are three primary phases occurring in the dehydration process: gypsum ($CaSO_4 \cdot 2H_2O$), bassanite ($CaSO_4 \cdot 0.5H_2O$) and γ-anhydrite (γ-$CaSO_4$), respectively. One consistent expression style (i.e., gypsum, bassanite and γ-anhydrite) was adopted in this study. As for the dehydration reaction, there are many controversial viewpoints for gypsum in the previously reported results. Some researchers think that the dehydration reaction can be divided into two step process from the starting gypsum to bassanite to γ-anhydrite. Previous thermo-Raman spectroscopy experiments by Chang et al. [10] have already disclosed that two-step dehydration reactions for gypsum were existed at temperatures of 298–573 K and room pressure. Their results indicated that gypsum transformed to bassanite at ~391 K, and then completely dehydrated to γ-anhydrite at ~473 K. More recently, Comodi et al. [11] investigated this dehydration reaction at 293–633 K and a pressure of ~2.5 GPa by Raman spectroscopy using a diamond anvil cell

* Corresponding author.
  E-mail address: dailidong@vip.gyig.ac.cn (L. Dai).

(DAC) , and found that gypsum still endure two-step dehydration reactions under high temperature and high pressure. In opposite, only one-step dehydration reaction is also observed in other previously reported work. Chio et al. [12] explored this investigation by Raman spectroscopy within 9–373 K and under room pressure. They observed that gypsum directly dehydrated to γ-anhydrite at ~373 K without the formation of intermediate bassanite. Mirwald [13] used a piston-cylinder high-pressure apparatus with the DPA technique to investigate the dehydration of gypsum, and reported that gypsum endured one-step dehydration reaction at the temperature of 293–353 K and pressure less than ~0.3 GPa.

In the present study, the Raman scattering spectra and electrical transport properties for gypsum were measured using a diamond anvil cell at conditions of 293–723 K and 0.3–12.2 GPa. At each correspondent pressure, the dehydration temperature was precisely determined. And furthermore, a phase diagram between the dehydration temperature and pressure was established at a wide temperature and pressure range.

2. Experimental procedure

The natural transparent gypsum single crystal was collected from Yuquan Diggings in Taiyuan city, Shanxi province. The samples were ground into powders using an agate mortar, and later baked at 308 K for 1 h in muffle furnace in order to remove the adsorbed water on the surfaces of the samples.

High-pressure Raman spectroscopy and electrical experiments were carried out using a diamond anvil cell (DAC) with an anvil culet of 300 μm. In the simultaneously high temperature and high pressure experiments, the external resistively heated DAC is used and a K-type thermocouple with an estimated accuracy of 5 K was used for temperature measurements. Raman spectroscopic measurements were performed using a Renishaw 2000 micro-confocal Raman spectrometer with a 514.5 nm argon ion laser. In

order to check the sulfate and water internal vibrational modes, Raman spectra were collected in the frequency shift range of 300–1200 cm^{-1} and in the 3000–3800 cm^{-1}, respectively. The ruby single crystal was selected to calibrate pressure through the wave number shift of the fluorescence peaks. In the heating process, the pressure was measured according to the high-temperature corrected equation of pressure calibration [14]. The electrical conductivity measurements were conducted using a Solartron-1260 impedance/gain phase analyzer at a given frequency range from 10^{-1} to 10^7 Hz. More details on the experimental procedures and measurement methods have been described previously [15–18].

3. Results and discussion

3.1. The phase transition at room temperature

Raman spectroscopy has been proved to be a sensitive probe for detecting pressure-induced structural phase transitions. Fig. 1 shows the Raman spectra of gypsum as a function of pressure at room-temperature condition. Below ~5.8 GPa, six typical Raman vibrational peaks for gypsum were observed at the frequency shift range of 300–1200 cm^{-1}, which is corresponding to the vibrational modes of the sulfate ion, i.e., v_1 (1006 cm^{-1}), v_2 (413 cm^{-1}), v_2 (493 cm^{-1}), v_3 (1134 cm^{-1}), v_4 (617 cm^{-1}), and v_4 (669 cm^{-1}). Meantime, two OH-stretching modes were also obtained, i.e., v_1 (3042 cm^{-1}) and v_3 (3492 cm^{-1}). All of these obtained characteristic peaks are good consistent with previous studies at atmospheric pressure and room temperature [10,19]. When the pressure is increased to ~5.8 GPa, a variation of the v_1 (SO$_4$) mode at 1006 cm^{-1} is observed: one obvious splitting phenomenon accompanies with two new separate new peaks at 1016 cm^{-1} and 1023 cm^{-1} (Fig. 1a). At the same time, two OH-stretching modes are suddenly broadened and weakened (Fig. 1b). During decompression, Raman spectra of gypsum is recoverable to its original state.
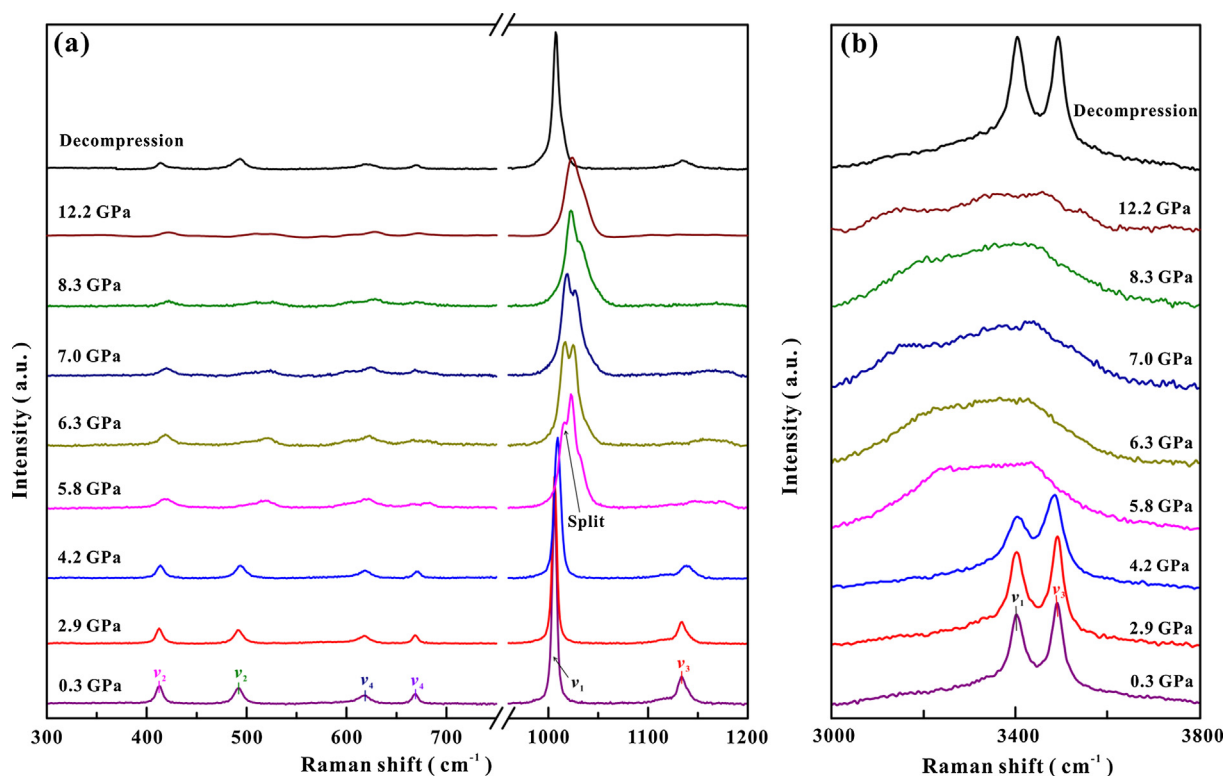

Fig. 1. (a) Raman spectra of gypsum in the SO$_4$ vibrational mode range (300–1200 cm^{-1}) under high pressure and room temperature. (b) Raman spectra of gypsum in the OH-stretching mode range (3000–3800 cm^{-1}) with increasing pressure.

In the present studies, we observed an occurrence of the structural phase transition for gypsum at ~5.8 GPa, which is characterized by these representative phenomena for the changes of the sulfate mode and as well as the hydroxyl stretching modes. In light of the variation from one individual to two independent new peaks in the splitting process of the v_1 (SO$_4$) mode, it is one efficient method in determining the occurrence of phase transition for gypsum at high pressure, which is also observed in the previous studies [6,7]. More specifically, the splitting of the v_1 (SO$_4$) mode indicates that sulfate tetrahedra in the crystal structure of gypsum endure a distortion during this phase transition. In addition, the sudden broadening and weakening of two OH-stretching modes provide another robust evidence for the phase transition at ~5.8 GPa. The broadening and weakening for two OH-stretching modes is characterized by the obvious change in the full-width at half-maximum (FWHM) as displayed in Fig. S1. Although we are unable to resolve two OH-stretching modes at ~5.8 GPa due to the broadening and weakening, it can still be seen that the v_1 (OH) and v_3 (OH) modes both rapidly shift to lower wave numbers at ~5.8 GPa, implying that the hydrogen bonding in the structure of gypsum is strengthened during this phase transition. And furthermore, this structural phase transition in gypsum is reversible, which is characterized by the recovery of Raman spectra during decompression.

Structural phase transition is often accompanied by the change of electrical properties at the same time. To further verify the phase transition in gypsum, pressure-induced electrical conductivity measurements were carried out up to ~12.2 GPa at atmospheric temperature. Fig. 2a displays the impedance spectra of gypsum obtained at pressure range of 0.3–12.2 GPa and room temperature. The impedance spectra exhibits one approximately semicircular arc at high frequencies and another small semicircular arc at low frequencies, and these respectively stand for the grain interior and grain boundary contribution. The pressure dependence of both the grain interior and boundary conductivity for gypsum at room temperature is displayed in Fig. 2b. One obvious inflexion point is observed at ~4.8 GPa. Below ~4.8 GPa, the grain interior and boundary electrical conductivity of gypsum both gradually increase with pressure. Above ~4.8 GPa, the grain interior and boundary conductivity for gypsum both decrease with pressure. The available discontinuity of the electrical conductivity at ~4.8 GPa is also indicative of a pressure-induced phase transition in

gypsum, which are good consistent with the results from our above-mentioned Raman spectra.

3.2. The dehydration reaction at high temperature

Raman spectroscopy has been widely applied to monitor the dehydration reaction of hydrous minerals owing to its advantage in identification of the composition and phase. Based on that, we monitored the variations of Raman modes of SO$_4$ and OH in gypsum to study the dehydration reaction at temperatures of 293–723 K and pressures of ~0.3, ~1.7, ~2.5, ~3.8, ~5.1, ~6.8, ~8.3 GPa. Fig. 3a and c display the Raman spectra for gypsum with increasing temperature at ~0.3 GPa. We only observe one critical temperature point (~473 K) from the changes of Raman shifts of six SO$_4$ modes and two OH-stretching modes (Fig. 3b and d). At ~473 K, the characteristic v_1 (SO$_4$) peak of gypsum which appears at around 1006 cm^{-1} suddenly shifts to 1024 cm^{-1}. At the same time, the OH-stretching peaks at 3402 cm^{-1} and 3492 cm^{-1} completely disappear. The appearance of new characteristic peak at ~1024 cm^{-1} and the disappearance of the OH-stretching modes can provide one strong evidence for the dehydration reaction for gypsum, which have been confirmed in the previous studies at atmospheric pressure and high temperature [12,19]. And furthermore, only one-step dehydration reaction from the starting gypsum to γ-anhydrite was observed at ~0.3 GPa. The recovered samples display three new Raman peaks at the positions under atmospheric pressure and room temperature: the v_1 (SO$_4$) at 1014 cm^{-1}, the v_1 (OH) at 3552 cm^{-1} and the v_3 (OH) at 3611 cm^{-1}, which all of these representative Raman modes are standing for the bassanite from the dehydration product of gypsum in the process of rehydration.

Raman spectra for gypsum are presented in Fig. 4a and c at conditions of ~2.5 GPa and 293–723 K. Two critical temperature points are obtained at ~523 and ~673 K from the typical variations of Raman shifts for six SO$_4$ modes and two OH-stretching modes (Fig. 4b and d). At ~523 K, Raman modes of SO$_4$ tetrahedra display obvious discontinuities, and meanwhile, two OH-stretching peaks at 3399 cm^{-1} and 3501 cm^{-1} change into one peak at 3553 cm^{-1}. The observed discontinuities of SO$_4$ modes and the appearance of a new peak at 3553 cm^{-1} are similar to previously reported results, and are indicative of the dehydration from gypsum to bassanite [11]. When the temperature is increased to ~673 K, the v_1 (SO$_4$)
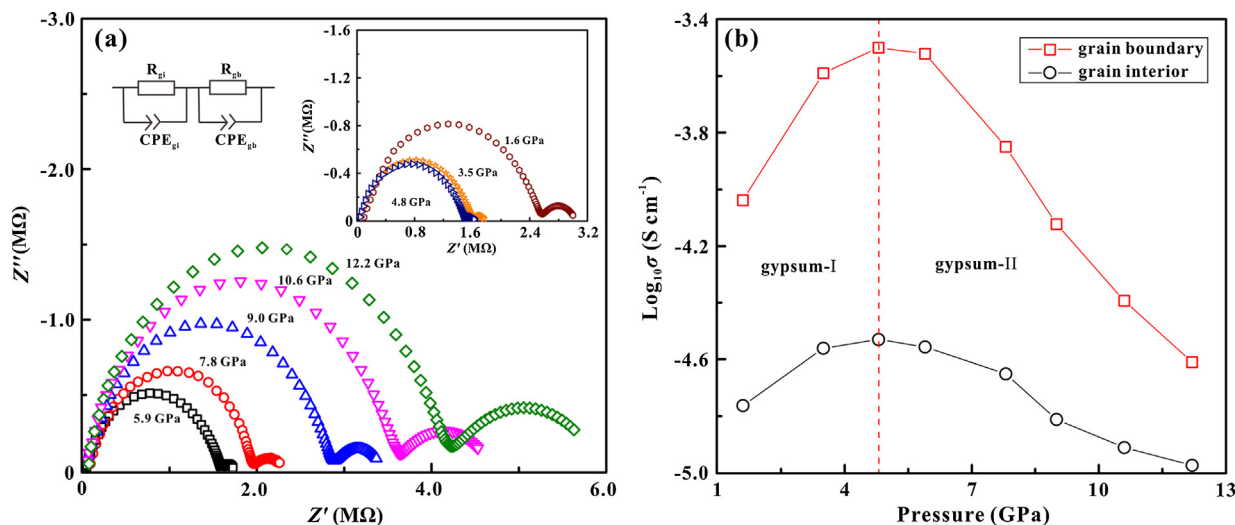

Fig. 2. (a) The impedance spectra of gypsum under high pressure and room temperature. (b) The grain interior and boundary electrical conductivity of gypsum with increasing pressure under room temperature.
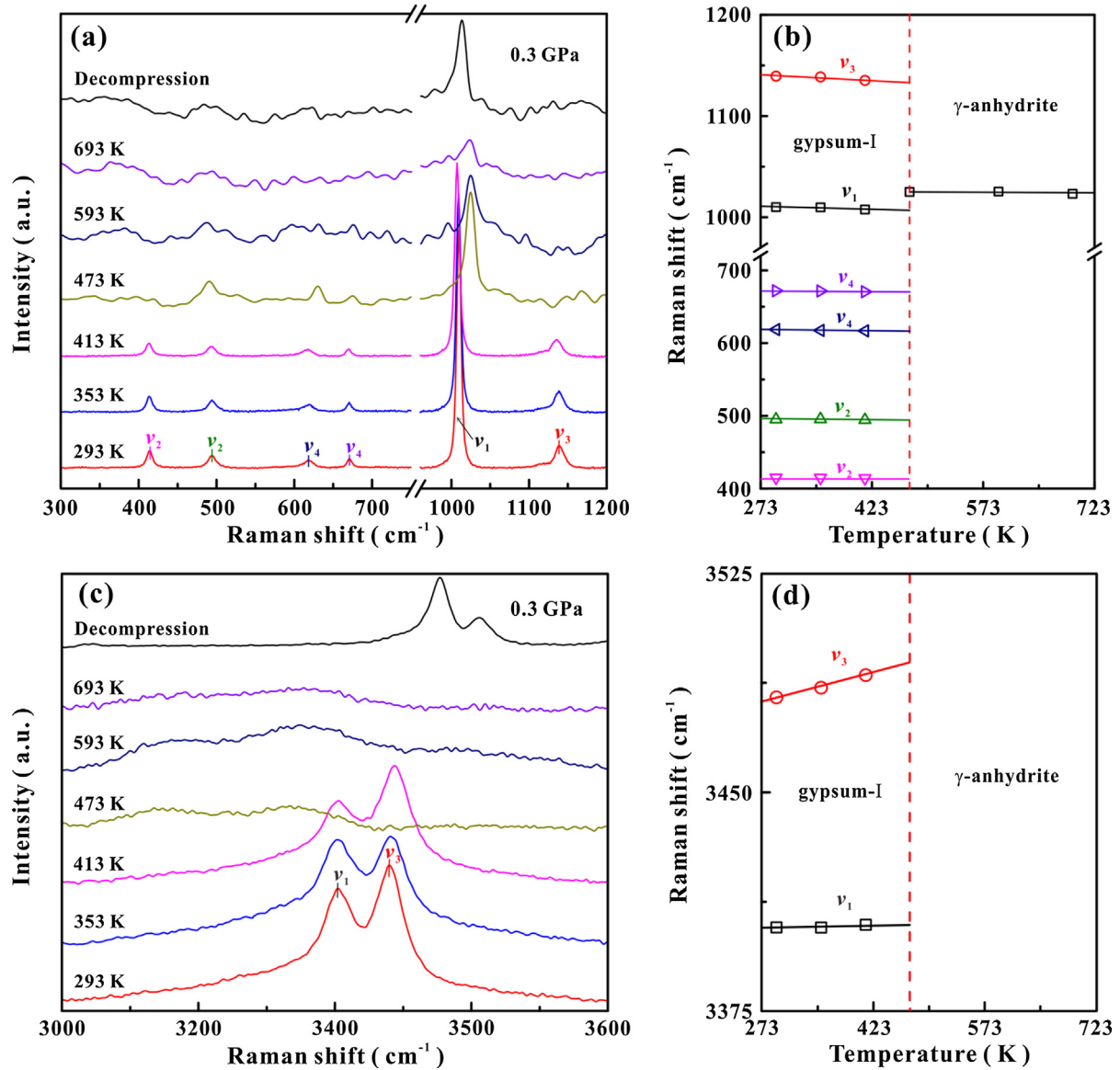
Fig. 3. (a) and (c) Raman spectra for gypsum with increasing temperature at ∼0.3 GPa in the SO_4 and OH-stretching mode ranges, respectively. (b) and (d) Raman shifts for gypsum collected between 273 K and 723 K at ∼0.3 GPa in the SO_4 and OH-stretching mode ranges, respectively. The straight lines serve as visual guides.

mode at 1013 cm^{-1} suddenly shifts to higher one at 1025 cm^{-1} and two OH-stretching modes completely disappear, indicating the dehydration from bassanite to γ-anhydrite. And furthermore, two-step dehydration reactions were confirmed from the starting gypsum to bassanite to γ-anhydrite at ∼2.5 GPa. The recovered samples display two new peaks at positions of 1014 cm^{-1} and 3555 cm^{-1} in Raman spectra at atmospheric pressure and room temperature, and the observed two new peaks belong to the representative Raman modes of bassanite forming in the process of rehydration of γ-anhydrite. The result at ∼1.7 GPa is similar to that at ∼2.5 GPa, gypsum transformed into bassanite at ∼513 K, and then completely dehydrated to γ-anhydrite at ∼593 K. As for the dehydration at another four pressures of ∼3.8, ∼5.3, ∼6.8 and ∼8.3 GPa, gypsum dehydrates to bassanite at ∼553, ∼573, ∼613 and ∼633 K respectively.

In terms of the dehydration reaction of gypsum, previously reported results on this issue are inconsistent. Some researchers consider that gypsum endure two-step dehydration reactions from the starting gypsum to bassanite to γ-anhydrite [10,11,19]. On the contrary, other previous work showed only one-step dehydration

reaction from the starting gypsum to γ-anhydrite [12,13,20]. In this present study, we confirmed that the dehydration of gypsum can be divided into two step process from gypsum to bassanite to γ-anhydrite at the pressure higher than ∼0.3 GPa (e.g., ∼1.7, ∼2.5, ∼3.8, ∼5.1, ∼6.8 and ∼8.3 GPa). As for the observed direct dehydration from gypsum to γ-anhydrite at a relatively lower pressure of ∼0.3 GPa, we attribute it to the effect of the rapid dehydration reaction from bassanite into γ-anhydrite, which causes that the formation of intermediate bassanite is not observed in our Raman spectroscopy experiments.

Many previous investigations have demonstrated that the dehydration temperature of hydrous minerals and rocks can be determined using the inflection point of the Arrhenius relation between electrical conductivity and temperature [21,22]. In order to further clarify the dehydration reaction at various pressures, the electrical conductivity experiments are conducted in an external heated DAC at 293–713 K and under high pressures of ∼2.5 and ∼8.1 GPa. Typical impedance spectra acquired at 293–713 K and ∼8.1 GPa are shown in Fig. 5a. The relationship between the logarithm of electrical conductivity and reciprocal temperature for
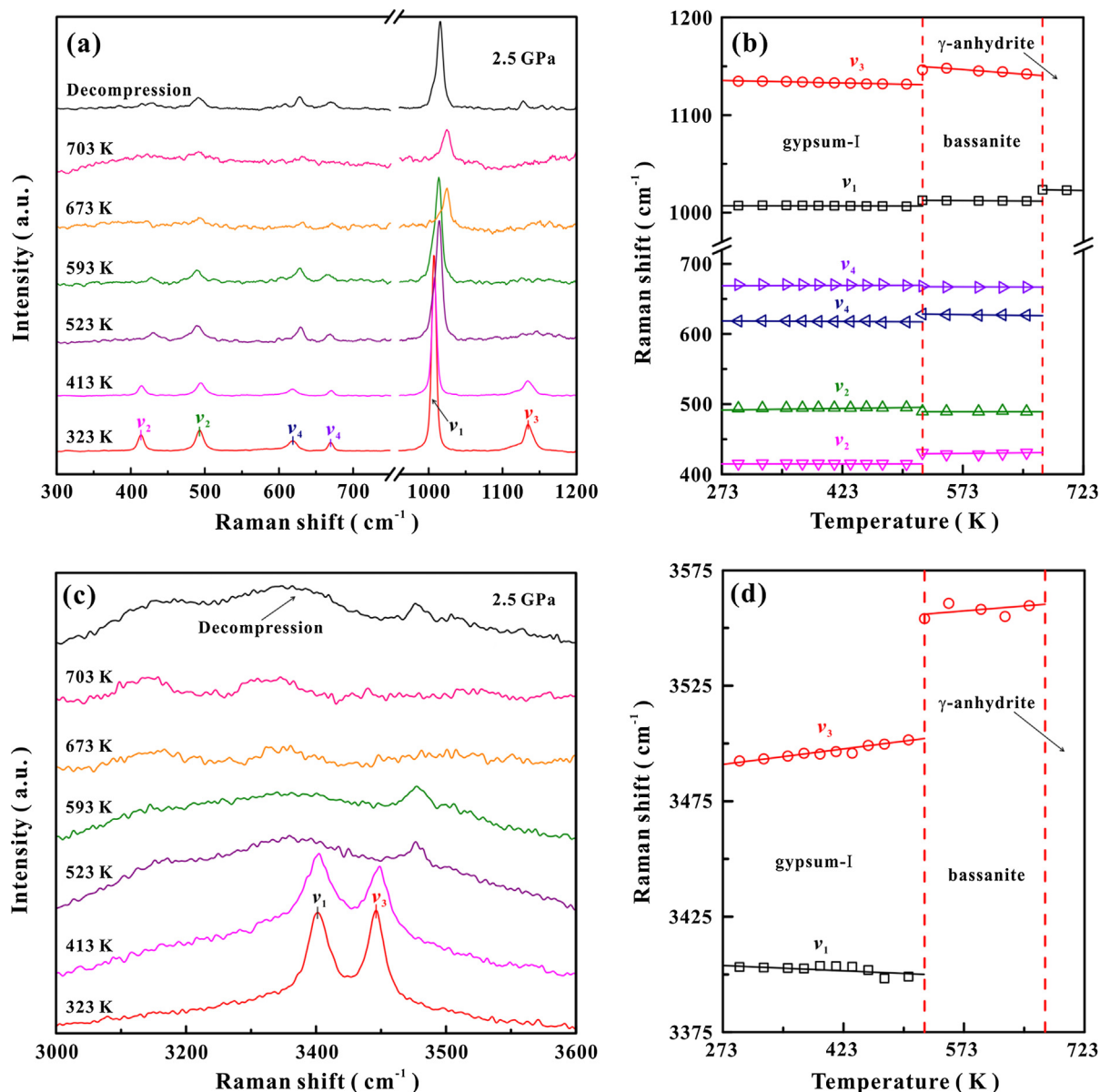
Fig. 4. (a) and (c) Raman spectra for gypsum with increasing temperature at ∼2.5 GPa in the SO_4 and OH-stretching mode ranges, respectively. (b) and (d) Raman shifts for gypsum collected between 293 K and 723 K at ∼2.5 GPa in the SO_4 and OH-stretching mode ranges, respectively. The straight lines serve as visual guides.

gypsum at ∼2.5 and ∼8.1 GPa is displayed in Fig. 5b. At ∼2.5 GPa, the electrical conductivity gradually increases in the temperature range from 293 K to 453 K, and then a sharp decrease in electrical conductivity is observed at ∼493 K. The conductivity increases with the rise of temperature at 493–593 K until another one sharp decrease in conductivity occurs at ∼633 K. According to the results of our Raman experiments carried out at pressure of ∼2.5 GPa, the first sharp decrease of electrical conductivity observed at ∼493 K is related to the dehydration reaction from gypsum to bassanite, and the second abrupt decrease in conductivity occurring at ∼633 K is related to the dehydration reaction from bassanite to γ-anhydrite. At ∼8.1 GPa, as presented in Fig. 5b, one abrupt decrease in the electrical conductivity is observed at ∼613 K, at which the conductivity of gypsum sharply decreases from 1.63×10^{-5} S/cm to 5.95×10^{-7} S/cm. The drop by nearly two orders of magnitude in conductivity is related to the breakdown of gypsum into bassanite and fluids. Our electrical conductivity results of ∼2.5 and ∼8.1 GPa indicates two-step dehydration reactions for gypsum, which is in good agreement with our obove-mentioned Raman results.

On the basis of the obtained dehydration temperature from Raman spectra data, we can establish a *P–T* phase diagram of gypsum at a relatively wide pressure range from 0.3 to 8.3 GPa, as shown in Fig. 6. At the same time, some comparisons with previously reported dehydration results on gypsum are also included [11,13,23]. There are some obvious discrepancies in the present dehydration temperature points and earlier results, which is possibly related to some influential factors, such as the rate of enhancing temperature, the humidity in the experimental environment and the concentration of impurity ion. The results from Nagase et al. [24] indicated that the heating rate has great effect on the dehydration temperature of hydrous sulphate minerals. Badens et al. [25] conducted an investigation of the influence of humidity on the dehydration for gypsum, and reported that the dehydration of gypusm under dry environment occurred at higher temperatures than that under wet environment. Jacques et al. [26] found that the dehydration temperature of waste gypsum is lower than that of pure gypsum, implying that the presence of impurity ion might lower the dehydration temperature for gypsum. And
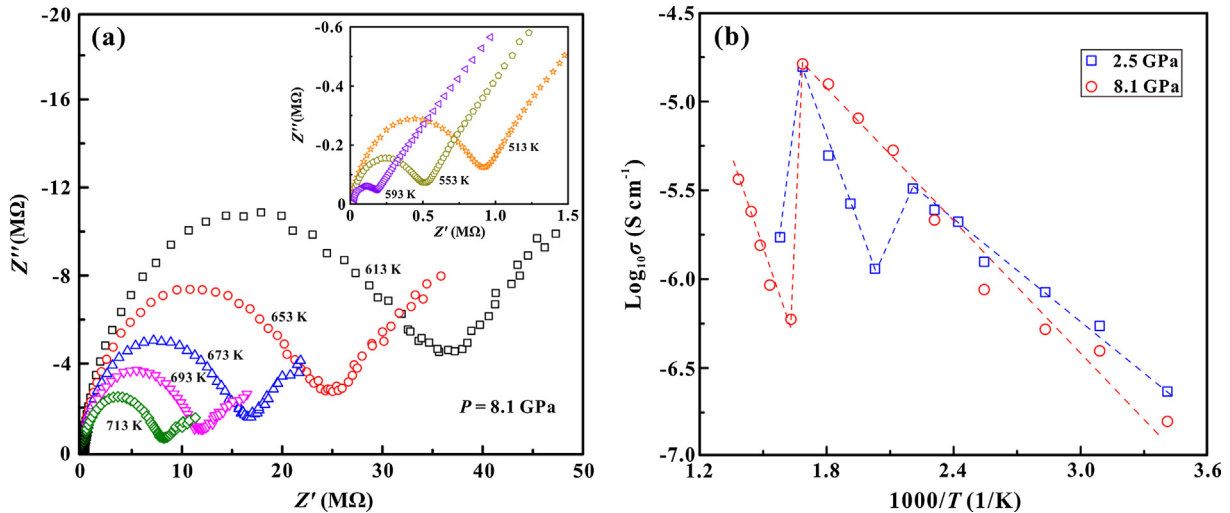
Fig. 5. (a) Representative impedance spectra of gypsum in the temperature range from 513 K to 713 K at ∼8.1 GPa. (b) Logarithm of electrical conductivity as a function of reciprocal temperature for gypsum at ∼2.5 and ∼8.1 GPa. Errors in conductivities and temperatures are smaller than the size of the symbols.
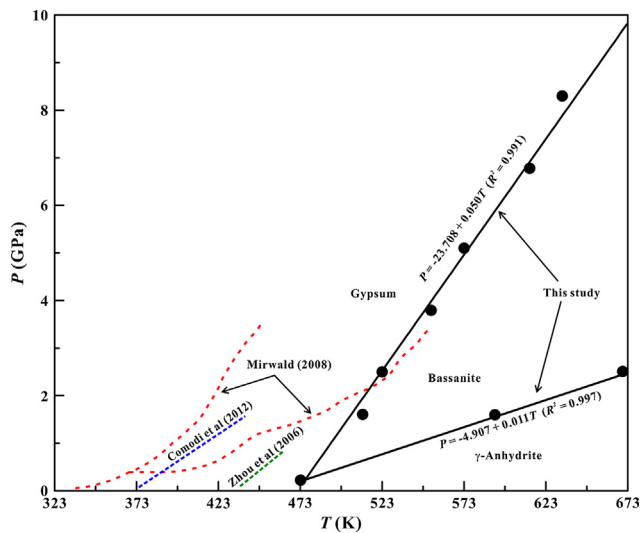

Fig. 6. Proposed P–T phase diagram of gypsum investigated at pressures up to ∼8.3 GPa and temperatures up to ∼723 K.

furthermore, according to the phase diagram in Fig. 6, the gypsum-bassanite and bassanite-anhydrite dehydration boundary are well determined to be P (GPa) = −23.708 + 0.050 T (K) and P (GPa) = −4.907 + 0.011 T (K), respectively, and the positive slopes of $\Delta P/\Delta T$ for two dehydration boundaries are in good agreement with previous wrok [13].

4. Conclusions

Raman spectroscopy and electrical conductivity experiments are conducted to study the structural phase transition and dehydration for gypsum at conditions of 0.3–12.2 GPa and 293–723 K using a diamond anvil cell. A structural phase transition in gypsum was confirmed at ∼5.8 GPa by virtue of the splitting of v_1 (SO_4) mode and one obvious discontinuity in the electrical conductivity at atmospheric temperature. The initial dehydration temperatures of gypsum at ∼0.3, ∼1.7, ∼2.5, ∼3.8, ∼5.1, ∼6.8 and ∼8.3 GPa corresponded to ∼473, ∼513, ∼523, ∼553, ∼573, ∼613 and ∼633 K respectively, which were determined by the variation in the SO_4 and OH Raman shifts and a sharp decrease of electrical conductiv-ity. At a relatively lower pressure of ∼0.3 GPa, only one-step dehydration reaction from the starting gypsum to γ-anhydrite was observed. As for the pressures higher than ∼0.3 GPa (e.g., ∼1.7, ∼2.5, ∼3.8, ∼5.1, ∼6.8 and ∼8.3 GPa), two-step dehydration reactions were confirmed from the starting gypsum to bassanite to γ-anhydrite. And furthermore, the $\Delta P/\Delta T$ slopes for the gypsum-bassanite and bassanite-anhydrite dehydration boundaries were determined to be 0.050 and 0.011 GPa/K, respectively.

Appendix A. Supplementary material

Supplementary data associated with this article can be found, in the online version, at https://doi.org/10.1016/j.cplett.2018.06.007.

References

[1] J.J. Wray, S.L. Murchie, S.W. Squyres, F.P. Seelos, L.L. Tornabene, Diverse aqueous environments on ancient Mars revealed in the southern highlands, Geology 37 (2009) 1043–1046, https://doi.org/10.1130/G30331A.1.

[2] R. Wirth, F. Kaminsky, S. Matsyuk, A. Schreiber, Unusual micro- and nano-inclusions in diamonds from the Juina Area, Brazil, Earth Planet. Sci. Lett. 286 (2009) 292–303, https://doi.org/10.1016/j.epsl.2009.06.043.

[3] G. Manthilake, N. Bolfan-Casanova, D. Novella, M. Mookherjee, D. Andrault, Dehydration of chlorite explains anomalously high electrical conductivity in the mantle wedges, Sci. Adv. 2 (2016) e1501631, https://doi.org/10.1126/sciadv.1501631.

[4] H. Leclère, D. Faulkner, J. Wheeler, E. Mariani, Permeability control on transient slip weakening during gypsum dehydration: Implications for earthquakes in subduction zones, Earth Planet. Sci. Lett. 442 (2016) 1–12, https://doi.org/10.1016/j.epsl.2016.02.015.

[5] H. Hu, L. Dai, H. Li, K. Hui, W. Sun, Influence of dehydration on the electrical conductivity of epidote and implications for high-conductivity anomalies in subduction zones, J. Geophys. Res. Solid Earth 122 (2017) 2751–2762, https://doi.org/10.1002/2016JB013767.

[6] E. Huang, J.A. Xu, J.F. Lin, J.Z. Hu, Pressure-induced phase transitions in gypsum, High Press. Res. 17 (2000) 57–75, https://doi.org/10.1080/08957950008200306.

[7] E. Knittle, W. Phillips, Q. Williams, An infrared and Raman spectroscopic study of gypsum at high pressures, Phys. Chem. Miner. 28 (2001) 630–640, https://doi.org/10.1007/s002690100187.

[8] P. Comodi, S. Nazzareni, P.F. Zanazzi, S. Speziale, High-pressure behavior of gypsum: a single-crystal X-ray study, Am. Mineral. 93 (2008) 1530–1537, https://doi.org/10.2138/am.2008.2917.

[9] L. Giacomazzi, S. Scandolo, Gypsum under pressure: a first-principles study, Phys. Rev. B 81 (2010) 064103, https://doi.org/10.1103/PhysRevB.81.064103.

[10] H. Chang, P.J. Huang, S.C. Hou, Application of thermo-Raman spectroscopy to study dehydration of $CaSO_4 \cdot 2H_2O$ and $CaSO_4 \cdot 0.5H_2O$, Mater. Chem. Phys. 58 (1999) 12–19, https://doi.org/10.1016/S0254-0584(98)00239-9.

[11] P. Comodi, A. Kurnosov, S. Nazzareni, L. Dubrovinsky, The dehydration process of gypsum under high pressure, Phys. Chem. Miner. 39 (2012) 65–71, https://doi.org/10.1007/s00269-011-0460-1.

[12] C.H. Chio, S.K. Sharma, D.W. Muenow, Micro-Raman studies of gypsum in the temperature range between 9 K and 373 K, Am. Mineral. 89 (2004) 390–395, https://doi.org/10.2138/am-2004-2-320.

[13] P.W. Mirwald, Experimental study of the dehydration reactions gypsum-bassanite and bassanite-anhydrite at high pressure: Indication of anomalous behavior of H_2O at high pressure in the temperature range of 50–300 °C, J. Chem. Phys. 128 (2008) 074502, https://doi.org/10.1063/1.2826321.

[14] S. Rekhi, L.S. Dubrovinsky, S.K. Saxena, Temperature-induced ruby fluorescence shifts up to a pressure of 15 GPa in an externally heated diamond anvil cell, High Temp.-High Press 31 (1999) 299–305, https://doi.org/10.1068/htrt161.

[15] Y. Zhuang, L. Dai, L. Wu, H. Li, H. Hu, K. Liu, L. Yang, C. Pu, Pressure-induced permanent metallization with reversible structural transition in molybdenum disulfide, Appl. Phys. Lett. 110 (2017) 122103, https://doi.org/10.1063/1.4979143.

[16] L. Dai, Y. Zhuang, H. Li, L. Wu, H. Hu, K. Liu, L. Yang, C. Pu, Pressure-induced irreversible amorphization and metallization with a structural phase transition in arsenic telluride, J. Mater. Chem. C 5 (2017) 12157–12162, https://doi.org/10.1039/C7TC03309E.

[17] L. Dai, K. Liu, H. Li, L. Wu, H. Hu, Y. Zhuang, L. Yang, C. Pu, P. Liu, Pressure-induced irreversible metallization accompanying the phase transitions in Sb2S3, Phys. Rev. B 97 (2018) 024103, https://doi.org/10.1103/PhysRevB.97.024103.

[18] K. Liu, L. Dai, H. Li, H. Hu, L. Wu, Y. Zhuang, C. Pu, L. Yang, Migration of impurity level reflected in the electrical conductivity variation for natural pyrite at high temperature and high pressure, Phys. Chem. Miner. 45 (2018) 85–92, https://doi.org/10.1007/s00269-017-0904-3.

[19] N. Prieto-Taboada, O. Gómez-Laserna, I. Martínez-Arkarazo, M.A. Olazabal, J.M. Madariaga, Raman spectra of the different phases in the $CaSO_4$-H_2O system, Anal. Chem. 86 (2014) 10131–10137, https://doi.org/10.1021/ac501932f.

[20] P.S.R. Prasad, V.K. Chaitanya, K.S. Prasad, D.N. Rao, Direct formation of the γ-$CaSO_4$ phase in dehydration process of gypsum: In situ FTIR study, Am. Mineral. 90 (2005) 672–678, https://doi.org/10.2138/am.2005.1742.

[21] W. Sun, L. Dai, H. Li, H. Hu, J. Jiang, K. Hui, Effect of dehydration on the electrical conductivity of phyllite at high temperatures and pressures, Miner. Petrol. 111 (2017) 853–863, https://doi.org/10.1007/s00710-017-0494-2.

[22] W. Sun, L. Dai, H. Li, H. Hu, L. Wu, J. Jiang, Electrical conductivity of mudstone (before and after dehydration at high P-T) and a test of high conductivity layers in the crust, Am. Mineral. 102 (2017) 2450–2456, https://doi.org/10.2138/am-2017-6146.

[23] X.Z. Zhou, H.F. Zheng, Q. Sun, In-situ Raman spectroscopic study of phase transition at high temperature and high pressure, Acta Petrol. Sin. 22 (2006) 3047–3052.

[24] K. Nagase, H. Yokobayashi, M. Kikuchi, K. Sone, Effects of heating rate (1–300° h^{-1}) on the non-isothermal thermogravimetry of $CuSO_4 \cdot 5H_2O$, Thermochim. Acta 35 (1980) 99–104, https://doi.org/10.1016/0040-6031(80)85027-1.

[25] E. Badens, P. Llewellyn, J.M. Fulconis, C. Jourdan, S. Veesler, R. Boistelle, F. Rouquerol, Study of gypsum dehydration by controlled transformation rate thermal analysis (CRTA), J. Solid State Chem. 139 (1998) 37–44, https://doi.org/10.1006/jssc.1998.7797.

[26] S.D.M. Jacques, A. Gonzalez-Saborido, O. Leynaud, J. Bensted, M. Tyrer, R.I.W. Greaves, P. Barnes, Structural evolution during the dehydration of gypsum materials, Min. Mag. 73 (2009) 421–432, https://doi.org/10.1180/minmag.2009.073.3.421.